Half-car model, finite element analysis and active control for vibrations of a truck concrete mixer

Ahmed Abu Hanieh

Department of Mechanical and Mechatronics Engineering,
Birzeit University, Palestine
Email: ahanieh@birzeit.edu

Abstract: This research focuses on the dynamic effect of vibrations caused by concrete mixer on the driver or passenger. The complete model for the concrete mixer is studied using finite element modelling technique through CATIA software. The most stringent vibrational mode on the passenger is the first mode at 73 rad/s (11.7 Hz), the second mode was found at 389 rad/s (62 Hz) and the third one at around 1,237 rad/s (197 Hz). The same system is simulated using MATLAB software based on half-car model and the same results with the same mode has been found which proves that the studied model is correct and representative. The integral force feedback (IFF) control technique is implemented here to damp and control the oscillations of the passenger's seat. IFF proved very high authority and robustness besides to its simplicity of use and implementation.

Keywords: half-car model; concrete mixer; finite element analysis; integral force feedback; IFF; active control; chassis; drum; vibration; mode; mode shape; frequency.

Reference to this paper should be made as follows: Hanieh, A.A. (2021) 'Half-car model, finite element analysis and active control for vibrations of a truck concrete mixer', *Int. J. Vehicle Noise and Vibration*, Vol. 17, Nos. 3/4, pp.289–302.

Biographical notes: Ahmed Abu Hanieh is a Professor in the Department of Mechanical and Mechatronics Engineering at Birzeit University since 2004 and worked as the Department Chairman for three years. He participated in more than 17 research and capacity building projects. He established and directed two master programs (Sustainable Engineering in Production and Renewable Energy Management). He acts as a Palestinian Higher Education Reforms Expert (HERE). He is a board member in the Higher Council for Innovation and Excellence in Palestine for six years. He is an author of two books, more than 20 journal articles and more than 30 conference papers. He is a volunteer reviewer for more than 17 international specialised journals and conferences.

1 Introduction

The first concrete mixer was invented 120 years ago in the beginning of the last century (Campbell, 1901), since then many patents with different designs have been registered around the world. Upon the spread of truck vehicles, designers started implementing and installing concrete mixers on top of truck to transport concrete from the plant to the building sites (Ball, 1930). One of the most dangerous problems facing concrete mixer's

truck drivers is the vibrations propagating from mixer, motor and ground into the driver cabin influencing the stability and health of the truck driver. Yan et al. (2012) have built a stochastic model for truck concrete mixer (TCM) under operation, this deterministic model is based on the study of network approach under stochastic travel time. Another model has been published by Braccesi and Landie (2009) for a fixed vertical planetary concrete mixer in which they calculated the induced force due to the mixing process in dry and wet phases. This study shows the influence of mixing forces on the design and angle of inclination of the mixing blades. The design and modelling of TCM blades is discussed in Fedorko et al. (2014) where the geometric design and kinematics of the mixer drum and blades are deeply calculated.

Abdel Fattah and Ruwanpura (2008) established an integrated computer aided design (CAD) and simulation model for the concrete operation. The complete operation was tackled here from cradle to grave by taking into account the concrete loading from concrete plant into the truck mixer, the on-road travel process of the truck and the onsite concrete pouring technique using truck mixer and truck pump. In highly dense urban areas there is a need to introduce an automated collection for the TCM operations to avoid mismatch and exhausting drivers (Lu et al., 2009). The authors here used cloud computing using GPS satellite to connect all moving mixers to a central computer at the headquarters of the concrete plant. Panasa and Pantouvakis (2013) discussed the simulation-based concrete truck mixers onsite batching plant using integrated definition models and calculations.

One of the main elements in modelling heavy trucks like TCM is modelling and stress calculations of the truck's chassis using FEM (Abd Rahman et al., 2008; Daraba et al., 2018). Saeed (1995) and Tan et al. (2014) discussed the concrete mixing process showing the charging and discharging processes due to drum rotation and its influence on the ready mixed concrete showing analytical equations and numerical values emphasising on the influence of the inclination angle of the blades and drum. Zhyhylii et al. (2018) studied the vibrations induced by the mixing process of toroidal mixing container, the rotating unbalance force is implemented here to represent the behaviour of the rotating concrete which an accepted procedure. Wankede and Sahu (2015) published a paper about the design and modification analysis of small concrete mixer with an electric motor showing the complete design and calculations of this mixer and proposing some modifications on its design for better operation. The design and modification of the shaft of the concrete mixer is also discussed by Wankede et al. (2016) using finite element methods. The dynamic behaviour and response of the concrete mixer drum was studied by Yang et al. (2017) considering that the drum is mounted on top of two spring- damper mounts, the effect of inclination angle, rotation speed and concrete level were tackled here as functions of the length of drum. The reduction gearbox used to rotate the concrete mixer drum is discussed in Yang et al. (2017), this gearbox consists of planetary gearbox mounted on top of the driving hydraulic motor driven by the hydraulic pump, the stress analysis of the same system was discussed by the same authors in Bae et al. (2015, 2018).

Electric buses are discussed in Zeng et al. (2019) where this article presents an analytical technique for the resonance sources of vibration transmission to an electric bus. These vibrations are amplified by the rear drive axle and thus are solved by adding a V-shaped bars to distribute the signals to the sides of the bus. Mohamad Qatu and co-authors discussed the problem of noise, vibration and harshness (NVH) in automotive engineering in Qatu et al. (2009) and Qatu (2012) concentrating on the different sources of vibration; power trains, road and tyre and wind related vibrations. They also discussed

the problem of brakes, chassis and electromechanical devices and their influence on vehicle vibrations. Qi et al. (2019a) presented using hydraulic and pneumatic systems with Fuzzy logic controllers to increase comfort and stability in a nine DOF vehicle. Another hydraulic suspension is presented in Wang et al. (2020), the suspension was tested in drop test for the vehicle and roll, pitch and pounce mode are studied using reduced degrees of freedom for the vehicle. The hydraulic suspension was tested by the same group on a two-axle bus as shown in Qi et al. (2019b), the lateral vibrations were tested here using lateral and roll dynamics for tuning of the suspension, a ten DOF lumped mass model was used in this reference and roll stiffness distribution ratio was used to tune the suspension.

This research is based on the modelling and simulation of a single rear and single steering axles TCM as shown in Figure 1. The system is represented by the CAD drawing in Figure 1(b) by replacing all springs and mounts with a leaf sheet of metal that has the equivalent stiffness in each case. The main contribution of this paper is the modelling technique that depends on half-car model and not quarter-car model as known in most of the previous literature. The mathematical model is compared to the finite element model that depends on the same technique. The IFF robust active control technique is used here to ensure stability of the system even when parameters change with time.

Figure 1 (a) Truck concrete mixer used in this research real photo and (b) CAD model (see online version for colours)

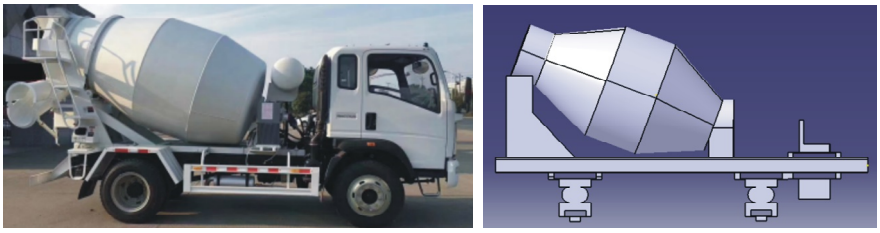

(a) (b)

2 Mathematical dynamic model

To understand the dynamic model of the TCM, consider the free body diagram shown in Figure 2 that represents a 2D half-car model for the TCM. Where the mixing drum and chassis are considered as complete unit (rigid body) which eliminated the relative motion between these parts considering that that are well attached without any losing parts, the mass of this part is denoted by the mass m_V and the centre of gravity of the whole vehicle is denoted by G. The drum and chassis are usually connected to each other via strong bands that assure very high stiffness between them which leads the assumption to consider them as one rigid body. The translational and rotational displacements of the vehicle (mixer + chassis) are x_V and θ respectively. The cabin and other vehicle components are taken-into-account in calculations as part of these ones. The passenger (driver) and his seat is denoted by the mass m_P, its dynamic displacement is x_P, the passenger's seat is mounted on a spring with a stiffness k_P and a viscous damper with a damping coefficient c_P and its distance from the centre of gravity is LPM.

Figure 2 Free body diagram for the truck concrete mixer (see online version for colours)

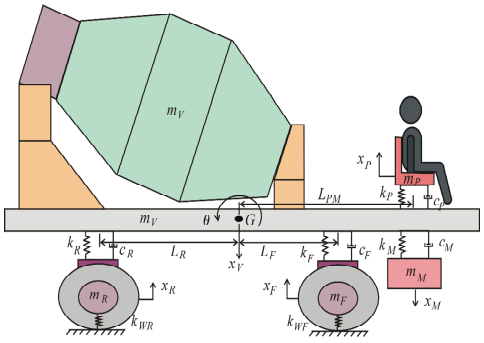

The internal combustion engine of the vehicle is denoted by the mass m_M, its dynamic displacement is x_M and it is located at a distance L_{PM} from the centre of gravity. The engine is mounted on spring with stiffness k_M and a viscous damper with a damping coefficient c_M. The front axle wheel is denoted by the mass m_F, its dynamic displacement is x_F and is located at a distance L_F from the centre of gravity G, the tyre rubber stiffness is denoted by k_{WF} and the whole wheel is mounted on a spring and damper k_F and c_F respectively that replace the leaf springs in the real truck. The rear axle wheel is denoted by the mass m_R, its dynamic displacement is x_R and is located at a distance L_R from the centre of gravity G, the tyre rubber stiffness is denoted by k_{WR} and the whole wheel is mounted on a spring and damper k_R and c_R respectively that replace the leaf springs in the real truck. All parts are considered rigid bodies and are coupled to each other by springs and dampers to simplify the mathematical linear calculations, only pitch and bounce modes are considered here (Chen et al., 2015).

The foregoing notations of the free body diagram will be used now to build the dynamic equations of motion knowing that using one dot on top of the variable means its first derivative with respect to time (velocity) and double dot means the second derivative with respect to time (acceleration).

The first equation of motion represents the linear translational dynamics of the front wheel and reads

$$m_F \ddot{x}_F = \left(-k_F - k_{WF}\right) x_F - c_F \dot{x}_F + k_F x_V + c_F \dot{x}_V + k_F L_F \theta + c_F L_F \dot{\theta} \tag{1}$$

The second equation of motion represents the linear translational dynamics of the rear wheel and reads

$$m_R \ddot{x}_R = \left(-k_R - k_{WR}\right) x_R - c_R \dot{x}_R + k_R x_V + c_R \dot{x}_V - k_R L_R \theta - c_R L_R \dot{\theta} \tag{2}$$

The third equation of motion represents the linear translational dynamics of the engine and reads

$$m_M \ddot{x}_M = -k_M x_M - c_M \dot{x}_M + k_M x_V + c_M x_V + k_M L_{PM} \theta + c_M L_{PM} \dot{\theta} - \left(\frac{1}{m_M}\right) F_M \tag{3}$$

The fourth equation of motion represents the linear translational dynamics of the passenger and reads

$$m_P\ddot{x}_P = -k_P x_P - c_P\dot{x}_P - k_P x_V - c_P\dot{x}_V - k_P L_{PM}\theta - c_P L_{PM}\dot{\theta} \tag{4}$$

The fifth equation of motion represents the linear translational dynamics of the whole vehicle (mixer + chassis) and reads

$$\begin{aligned} m_V\ddot{x}_V = {} & k_F x_F + c_F\dot{x}_F + k_R x_R + c_R\dot{x}_R + k_M x_M + c_M\dot{x}_M \\ & -k_P x_P - c_P\dot{x}_P - (k_F + k_R + k_M - k_P)x_V - (c_F + c_R + c_M - c_P)\dot{x}_V \\ & -(k_F L_F - k_R L_R + k_M L_{PM} - k_P L_{PM})\theta \\ & -(c_F L_F - c_R L_R + c_M L_{PM} - c_P L_{PM})\dot{\theta} - \left(\frac{1}{m_V}\right)F_C \end{aligned} \tag{5}$$

The sixth equation of motion represents the angular rotational dynamics of the whole vehicle (mixer + chassis) and reads

$$\begin{aligned} J\ddot{\theta} = {} & k_F L_F x_F + c_F L_F\dot{x}_F - k_R L_R x_R - c_R L_R\dot{x}_R + k_M L_{PM} x_M + c_M L_{PM}\dot{x}_M \\ & -k_P L_{PM} x_P - c_P L_{PM}\dot{x}_P - (k_F L_F - k_R L_R + k_M L_{PM} - k_P L_{PM})x_V \\ & -(c_F L_F - c_R L_R + c_M L_{PM} - c_P L_{PM})\dot{x}_V - (k_F L_F^2 + k_R L_R^2 + k_M L_{PM}^2 - k_P L_{PM}^2) \\ & -(c_F L_F^2 + c_R L_R^2 + c_M L_{PM}^2 - c_P L_{PM}^2)\dot{\theta} - \left(\frac{1}{J}\right)F_C \end{aligned} \tag{6}$$

where J is the mass moment of inertia of the whole system about the centre of gravity.

The system has been translated using state space approach to four matrices which makes it easier to handle such a six degrees of freedom system in MATLAB software. The state space equations are governed by:

$$\dot{e} = Ae + Bu \tag{7}$$

$$y = Ce + Du \tag{8}$$

The state variables vector e is selected as the following vector:

$$e = \left\{x_F\ \dot{x}_F\ x_R\ \dot{x}_R\ x_M\ \dot{x}_M\ x_P\ \dot{x}_P\ x_V\ \dot{x}_V\ \theta\ \dot{\theta}\right\}^T$$

The inputs vector u includes: the ground disturbance, engine disturbance and the disturbance force coming from the rotation of the concrete mixer drum. While the output vector y includes all the displacements of the passenger, engine, chassis and wheels.

The state space system reads the following matrices:

A system matrix

B input matrix

C output matrix

D feedthrough matrix.

$$
A = \begin{bmatrix}
0 & 0 & 0 & 0 \\
(-k_{WF} - k_F)/m_F & -c_F/m_F & 0 & 0 \\
0 & 0 & 0 & 1 \\
0 & 0 & (-k_{WR} - k_R)/m_R & -c_R/m_R \\
0 & 0 & 0 & 0 \\
0 & 0 & 0 & 0 \\
0 & 0 & 0 & 0 \\
0 & 0 & 0 & 0 \\
0 & 0 & 0 & 0 \\
k_F/m_V & c_F/m_V & k_R/m_V & c_R/m_V \\
0 & 0 & 0 & 0 \\
k_F L_F/J & c_F L_F/J & -k_R L_R & -c_R L_R/J
\end{bmatrix}
$$

$$
\begin{bmatrix}
0 & 0 & 0 & 0 \\
0 & 0 & 0 & 0 \\
0 & 0 & 0 & 0 \\
0 & 0 & 0 & 0 \\
0 & 0 & 0 & 0 \\
-k_M/m_M & 0 & 0 & 0 \\
0 & 0 & 0 & 1 \\
0 & -c_M/m_V & -k_p/m_p & -c_p/m_p \\
0 & 0 & 0 & 0 \\
k_M/m_V & c_M/m_V & -k_p/m_V & -c_p/m_V \\
0 & 0 & 0 & 0 \\
k_M L_{pM} & cL_{pM}/J & -k_p L_{pM}/J & -c_p L_{pM}/J \\
0 & 0 & 0 & 0 \\
k_F/L_F & c_F/L_F & k_F L_F/m_F & c_F L_F/m_F \\
0 & 0 & 0 & 0 \\
k_R/m_R & c_R/m_R & -k_R L_R/m_R & -c_R L_R/m_R \\
0 & 0 & 0 & 0 \\
k_M/m_M & c_M/m_M & k_M L_{PM}/m_M & c_p L_{pM}/m_M \\
0 & 0 & 0 & 0 \\
-k_p/m_p & c_p/m_p & -k_p L_{pM}/m_p & -k_p L_{pM}/m_p \\
0 & 1 & 0 & 0 \\
I & II & III & IV \\
0 & 0 & 0 & 1 \\
i & ii & iii & iv
\end{bmatrix}
$$

where

$$I = -(k_F + k_R + k_M - k_P)/m_V$$

$$II = -(c_F + c_R + c_M - c_P)/m_V$$

$$III = -(L_F k_F - L_R k_R + L_{PM} k_M - L_{PM} k_P)/m_V$$

$$IV = (L_F c_F - L_R c_R + L_{PM} c_M - L_{PM} c_P)/m_V$$

$$i = -(L_F k_F - L_R k_R + L_{PM} k_M - L_{PM} k_P)/J$$

$$ii = -(L_F c_F - L_R c_R + L_{PM} c_M - L_{PM} c_P)/J$$

$$iii = -\left(L_F^2 k_F + L_R^2 k_R + L_{PM}^2 k_M - L_{PM}^2 k_P\right)/J$$

$$iv = -\left(L_F^2 c_F + L_R^2 c_R + L_{PM}^2 c_M - L_{PM}^2 c_P\right)/J$$

$$B = \begin{bmatrix}
0 & 0 & 0 & 0 & 0 \\
(-k_F - k_{WF}) & 0 & 0 & 0 & 0 \\
0 & 0 & 0 & 0 & 0 \\
0 & (-k_R - k_{WR})/m_R & 0 & 0 & 0 \\
0 & 0 & 0 & 0 & 0 \\
0 & 0 & -1/m_M & 0 & 0 \\
0 & 0 & 0 & 0 & 0 \\
0 & 0 & 0 & 0 & 0 \\
0 & 0 & 0 & 0 & 0 \\
k_F/m_V & k_R/m_V & 0 & -1/m_V & -(k_F + k_R + k_M - k_p)/m_V \\
0 & 0 & 0 & 0 & 0 \\
k_F/L_F/J & k_R L_R/J & 0 & -k_R/J & -(k_F L_F + k_R L_R + k_M L_{pM})/J
\end{bmatrix}$$

$$C = \begin{bmatrix}
1 & 0 & 0 & 0 & 0 & 0 & 0 & 0 & 0 & 0 & 0 & 0 \\
0 & 0 & 1 & 0 & 0 & 0 & 0 & 0 & 0 & 0 & 0 & 0 \\
0 & 0 & 0 & 0 & 1 & 0 & 0 & 0 & 0 & 0 & 0 & 0 \\
0 & 0 & 0 & 0 & 0 & 0 & 1 & 0 & 0 & 0 & 0 & 0 \\
0 & 0 & 0 & 0 & 0 & 0 & 0 & 0 & 1 & 0 & 0 & 0 \\
0 & 0 & 0 & 0 & 0 & 0 & 0 & 0 & 0 & 0 & 1 & 0 \\
0 & 0 & 0 & 0 & 0 & 0 & k_p & c_p & -k_p & -c_p & 0 & 0
\end{bmatrix}$$

$$D = \begin{bmatrix} 1 & 0 & 0 & 0 & 0 \\ 0 & 1 & 0 & 0 & 0 \\ 0 & 0 & 0 & 0 & 0 \\ 0 & 0 & 0 & 0 & 0 \\ 0 & 0 & 0 & 0 & 1 \\ 0 & 0 & 0 & 0 & 0 \\ 0 & 0 & 0 & 0 & 0 \end{bmatrix}$$

3 Finite element model

A finite element model (FEM) for the concrete mixer was made using CATIA software. The FEM mesh contains 9,894 nodes and 41,988 tetrahedron elements. Constraints have been added to the different parts of the mixer model to restrict all directions except vertical translation and rotation about in-page direction to obtain a 2D behaviour for the model. Figure 3 shows the Von Mises stresses on the outer most surface of each part resulting from the static analysis, the maximum values of stress is 716 MPa that appears at the leaf springs holding the wheels. Figure 3 shows that this maximum stress is concentrated only on the leaf springs and we know that the spring steel out of which the leaf springs are made is equal to 1,300 MPa which means that still we have a factor of safety of around 2. For the other components the factor of safety is much higher. The static load added to the mixer drum was 13,500 kg which represents 6 m^3 of concrete mounted on a rigid drum connected rigidly to the chassis leading to have the flexibility of the low frequency modes caused by the stiffness of the leaf springs. The deformation of these springs forms the first vibrational mode and appoints the most dangerous points exposed to failure due to continuous usage of the vehicle. The number of degrees of freedom and number of elements of the FEM have been reduced to simplify the analysis and reduce the simulation time (Chen et al., 2014; Tan, 2020).

Figure 3 Von Mises stresses of the concrete mixer (see online version for colours)

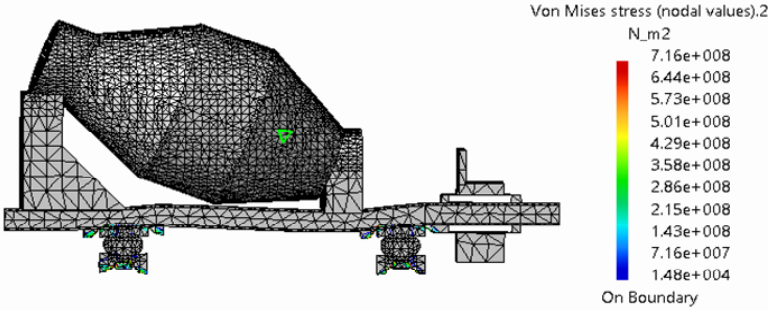

The dynamic frequency analysis for the same system with the same mesh and same boundary conditions. Figure 4 shows the first three modes and mode shapes of the system. The first vibrational mode at 73.5 rad/s (11.7 Hz) is the bounce mode representing the oscillational motion in the vertical direction equally on both wheels. This mode is caused by the flexibility of the steel leaf springs holding the vehicle's suspension

and the stiffness of the tyres made of rubber. The main sources of these oscillations are the road corrugations and the rotational speed of the mixer drum that rates around 20 rpm. The second mode is the vertical oscillations of the frontal part of the chassis at a frequency of 389 rad/s (62 Hz). The main source of this mode is the oscillations of the tyres and leaf springs of the frontal axle wheels. The third mode at 1,237 rad/s (197 Hz) that affects the passenger's seat and the motor mount. The main source of these oscillations is the dynamics of the diesel engine of the vehicle that lies under the passenger's seat. Therefore, its effect influences the passenger directly.

Figure 4 Vibration first three modes and mode shapes, (a) mode 1 = 73 rad/s = 11.7 Hz (b) mode 2 = 389 rad/s = 62 Hz (c) mode 3 = 1,237 rad/s = 197 Hz (see online version for colours)

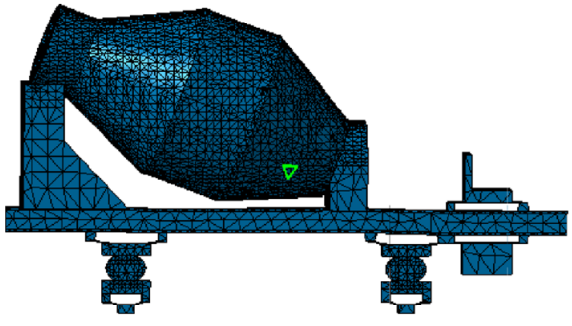

(a)

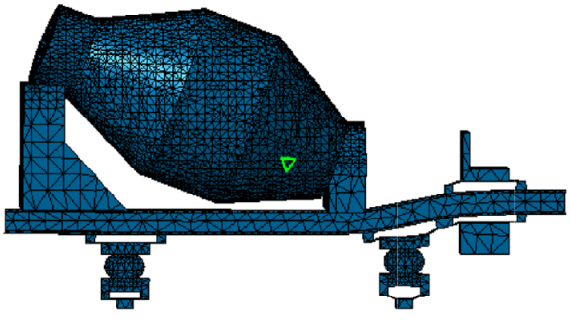

(b)

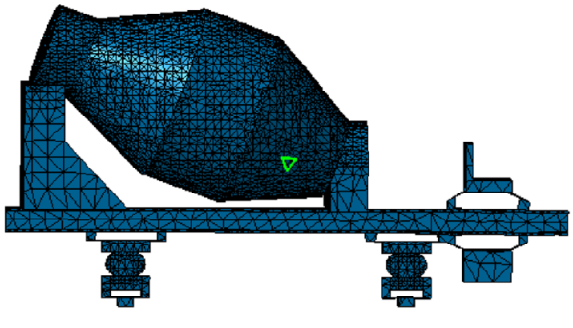

(c)

4 Simulation of the dynamic model

Implementing the foregoing 4 matrices A, B, C and D in MATLAB software results in the identification of the system. The most important influence tackled here is the influence of the vibration disturbance inputs on the passenger or driver of the truck. Figure 5 represents two frequency response functions (FRF) where the large FRF represents the transfer function between the chassis disturbance propagating through the seat mount and the displacement of the passenger's seat itself, forming a displacement transmissibility function. The first vibrational mode here appears at 73 rad/s (11.6 Hz) which is the vertical bounce mode of the vehicle on both wheels equally causing vertical oscillations for the whole vehicle.

The second mode is at 383 rad/s (61 Hz) and represents the influence of the chassis vibrations on the passenger's seat and the third is at around 1,250 rad/s (200 Hz) and represents the influence of the engine motor on the passenger's seat.

The small FRF on the corner depicts the displacement response of the chassis relative to the ground disturbance. It is obvious that this plot does not show the first mode because it corresponds to the vibration of the passenger.

Figure 5 FRF between the chassis displacement as an input and the passenger's displacement as an output and the FRF of the chassis versus the ground (see online version for colours)

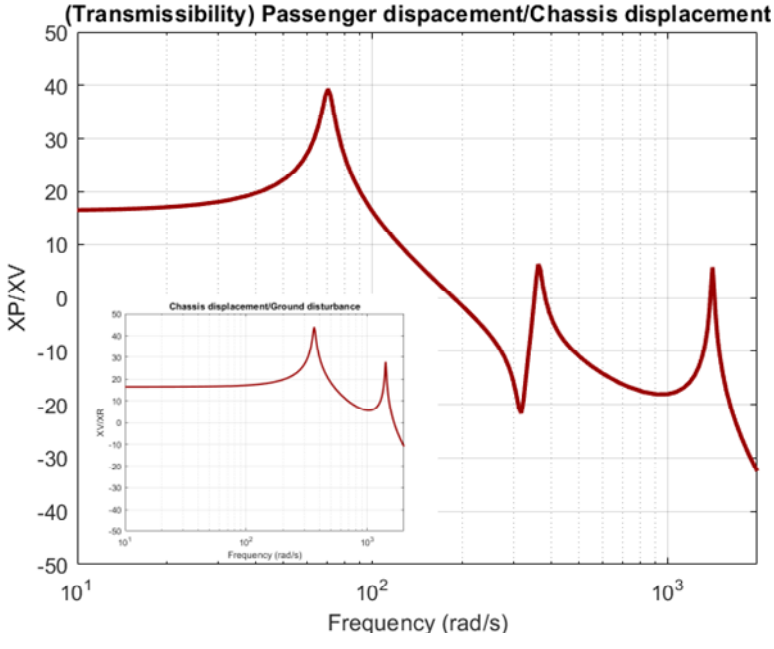

5 Active control technique

It has been mentioned so far that the required here is to control or isolate the passenger's seat from the propagating vibrations that dominate the comfort of the driver, in many circumstances it causes severe damage to his nerves and brain. The proposed control

technique is based on damping and isolating the passenger from the surrounding disturbance. This can be done by using the IFF control technique. Andre Preumont has discussed deeply with many examples the effect of the IFF controller (Preumont, 2002), he has proved that the IFF control technique is a robust controller with very high authority on low frequency vibration modes and stable even when there is an appendage connected to the system (Preumont et al., 2002). Therefore, it has been used here to damp the first vibration mode influencing the passenger of the concrete mixer. The technique is based on measuring the total force propagating from the chassis to the seat and feeding it back to a force voice coil actuator under the seat used to oppose that force. The total force coming to the seat FP reads:

$$F_P = k_P\left(x_V - x_P\right) + c_P\left(\dot{x}_V - \dot{x}_P\right) \tag{9}$$

This force is measured by a force sensor, it represents the relative spring force and the relative damper force caused by the dynamic oscillations of the chassis. The force is conditioned and processed by the simple integrator and multiplied by a specific gain then it is fed back to a voice coil electromagnetic actuator installed under the seat. The equation governing this control technique is depicted in equation (10)

$$F_a = -g\frac{1}{s}F_P \tag{10}$$

where F_a is the force exerted by the actuator on the seat and g is the gain of the controller. MATLAB-Simulink is used to simulate the authority of the control system on the whole system. The closed-loop system behaviour is verified using the root-locus technique. The IFF controller had an impact only on the first mode at 73 rad/sec (11.7 Hz) where one can see from the root locus plot shown in Figure 6 that implementing the IFF controller adds a pole at the origin and by increasing the controller gain g the first poles migrates from its undamped position towards the real axis till reaching critical damping position causing a very high stability for the seat, while it has no effect on the other modes.

Figure 6 Root-locus for the closed-loop system (see online version for colours)

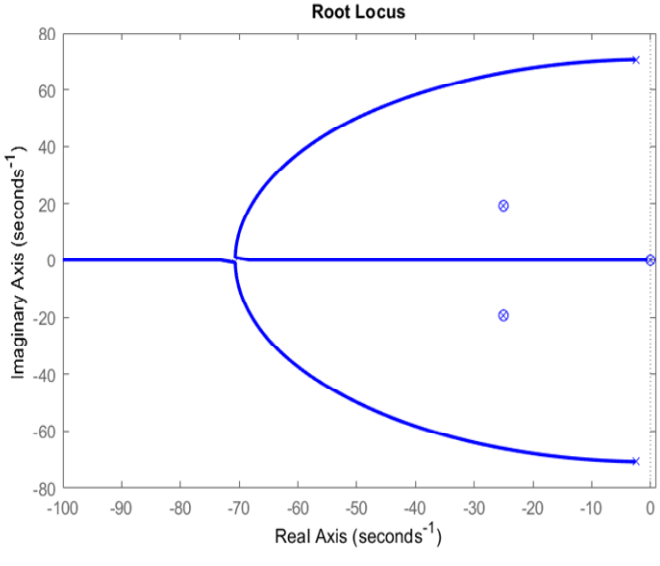

The overall authority of the controller is shown in Figure 7 where the frequency response shows the transmissibility FRF taking the ground disturbance as an input and the passenger's seat displacement as an output. The plot shows that the controller was able to reduce the seat's response 10 times (20 dB) by using a gain equals to 20 units only. The plot does not show any authority for the controller on the other vibration modes and this is logic because the other modes correspond to the chassis oscillations that cannot be regulated by this controller. The time response of the passenger's seat displacement with and without control is shown in Figure 7 as well on the lower left corner. Time response shows that the settling time for the oscillations has been reduced by the controller from 2 seconds to 0.5 second which is a very significant effect.

Figure 7 Transmissibility FRF between passenger's displacement and ground disturbance and a plot for the time response for passenger's seat (see online version for colours)

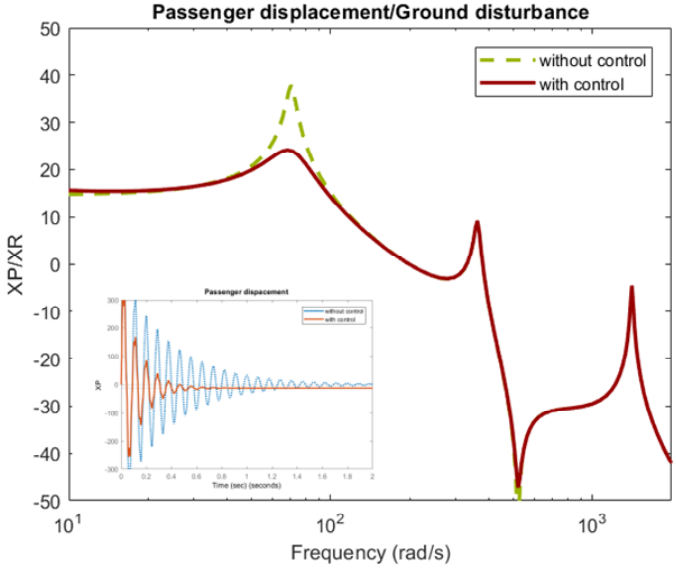

6 Conclusions

The foregoing article discussed the influence of vibrations of a TCM on its driver, these vibrations are cause by three main sources; the corrugations of the road, the unbalance of the diesel engine and the rotation of the concrete drum. This disturbance propagates into the passenger's body causing un-comfort driving period specially that the driver spends hours and hours behind the steering wheel in un-comfortable conditions. The truck with mixer has been represented mathematically as a half-car model by six second order linear differential equations, these equations were translated to matrix form through state space approach and MATLAB was used to estimate the frequency and time response of the different parts. The planar half-car system was modelled again using Catia software by finite element method, static and dynamic frequency analysis were made for the system and the results were illustrated showing the von Mises stress analysis and the vibrational modes and mode shapes. The mathematical model and the finite element model were

compared and proved high similarity which means that the model is correct and validated in two ways. IFF control technique was implemented on the system to suppress and eliminate the disturbance dominating the passenger's seat, this control technique proved to have high authority and robustness in the vicinity of the first vibrational mode removing the overshoot of that mode and keeping the high frequency attenuation unaffected.

References

Abd Rahman, R., Tamin, M. and Kurdi, O. (2008) 'Stress analysis of heavy-duty truck chassis as a preliminary data for its fatigue life prediction using FEM', *Jurnal Mekanikal*, December, No. 26, pp.76–85.

Abdel Fattah, A. and Ruwanpura, J. (2008) 'An integrated CAD and simulation model for concrete operations', *Proceedings of the 2008 Winter Simulation Conference*.

Bae, M., Bae, T. and Kim, D. (2018) 'The strength analysis of differential planetary gears of gearbox for concrete mixer truck', *4th International Conference on Advanced Engineering and Technology* (4th ICAET) *IOP Publishing IOP Conf. Series: Materials Science and Engineering*, p.317.

Bae, M., Bae, T., Cho, Y., Son, H. and Kim, D. (2015) 'The stress analysis of planetary gear system of mixer reducer for concrete mixer truck', *Journal of Drive and Control*, Vol. 12, No. 4, pp.77–81.

Ball, C. (1930) *Concrete Mixer and Agitator*, US-Patent No. 1,781,965, Wisconsin.

Braccesi, C. and Landi, L. (2009) 'An analytical model for force estimation on arms of concrete mixers', *Proceedings of the ASME 2009 International Design Engineering Technical conferences and Computers and Information in Engineering Conference IDETC/CIE 2009*, August 30 – September 2, 2009, San Diego, California, USA.

Campbell, H. (1901) *Concrete Mixer*, US-Patent No. 670,222, New York.

Chen, Y., Zhang, B. and Chen, S. (2014) 'Model reduction technique tailored to the dynamic analysis of a beam structure under a moving load', *Shock and Vibration*, Vol. 2014, No. 406093, p.13.

Chen, Y., Zhang, B., Zhang, N. and Zheng, M. (2015) 'A condensation method for the dynamic analysis of vertical vehicle–track interaction considering vehicle flexibility', *Journal of Vibration and Acoustics*, Vol. 37, No. 4, pp.041010-1–041010-8.

Dărabă, C., Ungureanu, N. and Dărabă, D. (2018) 'Checking the truck chassis after the repair process', *Scientific Bulletin, Serie C, Fascicle: Mechanics, Tribology, Machine Manufacturing Technology*, ISSN, Vol. 2018, No. 32, pp.1224–3264.

Fedorko, G., Kral, Jr. Kral, J., Ristovic, I. and Molnar, V. (2014) 'Determination of calculation for shape of blades trace in the concrete mixer truck', *8th International Conference Interdisciplinary in Engineering, INTER-ENG 2014*, Tirgue-Mures, Romania.

Lu, M., ASCE, M., Shen, X. and Chen, W. (2009) 'Automated collection of mixer truck operations data in highly dense urban areas', *Journal of Construction Engineering and Management*, Vol. 135, No. 117, pp.17–23.

Panasa, A. and Pantouvakis, J.P. (2013) 'Simulation-based concrete truck-mixers fleet size determination for on-site batch plant operation', *Procedia - Social and Behavioral Sciences*, Vol. 74, pp.459–467.

Preumont, A. (2002) *Vibration Control of Active Structures*, 2nd ed., Kluwer Academic Publishers, Brussels.

Preumont, A., Francois, A., Bossens, F. and Abu Hanieh, A. (2002) 'Force feedback versus acceleration feedback in active vibration isolation', *Journal of Sound and Vibration*, October, 2002, Vol. 257, No. 4, pp.605–613, Elsevier.

Qatu, M. (2012) 'Recent research on vehicle noise and vibration', *International Journal of Vehicle Noise and Vibration*, Vol. 8, No. 4, pp.289–301.

Qatu, M., Abdelhamid, M., Pang, J. and Sheng, G. (2009) 'Overview of automotive noise and vibration', *International Journal of Vehicle Noise and Vibration*, Vol. 5, Nos. 1–2, pp.1–35.

Qi, H., Chen, Y., Zhang, N., Zhang, B., Wang, D. and Tan, B. (2019a) 'Improvement of both handling stability and ride comfort of a vehicle via coupled hydraulically interconnected suspension and electronic controlled air spring', *Journal of Automobile Engineering*, Vol. 234, Nos. 2–3, pp.1–20.

Qi, H., Zhang, B., Zhang, N., Zheng, M. and Chen, Y. (2019b) 'Enhanced lateral and roll stability study for a two-axle bus via hydraulically interconnected suspension tuning', *SAE Int. J. Veh. Dyn., Stab., and NVH*, Vol. 3, No. 1, pp.5–18.

Saeed, K. (1995) 'Technique of multi-step concrete mixing', *Materials and Structures*, Vol. 28, No. 4, pp.230–234.

Tan, B., Chen, Y., Liao, Q., Zhang, B., Zhang, N. and Xie, Q. (2020) 'A condensed dynamic model of a heavy-duty truck for optimization of the powertrain mounting system considering the chassis frame flexibility.', *Journal of Automobile Engineering*, Vol. 234, Nos. 10–11, pp.2602–2617.

Tan, Y., Deng, R., Feng, Y., Zhang, H. and Jiang, S. (2014) 'Numerical study of concrete mixing transport process and mixing mechanism of truck mixer', *Engineering Computations: International Journal for Computer – Aided Engineering and Software*, Vol. 32, No. 4, pp.1041–1065.

Wang, M., Zhang, B., Chen, Y., Zhang, N. and Zhang, J. (2020) 'Frequency-based modeling of a vehicle fitted with roll-plane hydraulically interconnected suspension for ride comfort and experimental validation', *IEEE Access*, Vol. 8, pp.1091–1104.

Wankhede, A. and Sahu, A. (2015) 'Design, modification and analysis of concrete mixer machine', *International Journal on Recent and Innovation Trends in Computing and Communication*, Vol. 3, No. 12.

Wankhede, A., Sahu, A. and Gulhane, U. (2016) 'Design, modification and analysis of shaft of concrete mixer machine', *International Journal for Research and Development in Technology*, Vol. 6, No. 4, pp.6613–6616.

Yan, S., Lin, H.C. and Jiang, X.Y. (2012) 'A planning model with a solution algorithm for ready mixed concrete production and truck dispatching under stochastic travel times', *Engineering Optimization*, Vol. 44, No. 4, pp.427–447.

Yang, J., Zeng, H., Zhu, T. and An, Q. (2017) 'Study on the dynamic performance of concrete mixer's mixing drum', *Mech. Sci*., Vol. 8, No. 1, pp.165–178.

Zeng, M., Tan, B., Ding, F., Zhang, B., Zhou, H. and Chen, Y. (2019) 'An experimental investigation of resonance sources and vibration transmission for a pure electric bus', *Journal of Automobile Engineering*, Vol. 234, No. 4, pp.1–13.

Zhyhylii, S., Kharchenk, M. and Katella, J. (2018) 'Mathematical model of the dynamic action of the controlled vibration exciter on the processed medium of mixer with toroidal working container', *International Journal of Engineering and Technology*, Vol. 7, Nos. 3.2, pp.478–485.